



Assessment of GNSS and Map Integration for Lane-Level Applications in the Scope of Intelligent Transportation Location Based Services (ITLBS)

Emerson Pereira Cavalheri and Marcelo Carvalho dos Santos

Abstract

To enable safe and robust Intelligent Transportation Systems (ITS) applications, the integration of different sensors and techniques will certainly be a common reality. One application in this context is the lane-keeping techniques for autonomous driving systems. These systems normally use imagery sensors for lane identification, however imagery systems always depend on light and well-structured roads. One potential worldwide autonomous driving technique without any other lane and road detection/identification sensor would be GNSS positions along with accurate map information. However, this fusion depends on the accuracy and reliability of both GNSS positions and map information. The positioning accuracy that Intelligent Transportation Location Based Services (ITLBS) requires for where-in-lane and active control applications are 0.5 m and 0.1 m, respectively. To evaluate the potential of fusion, this work proposes an integration of GNSS and map information in the attempt to address the lane-keeping problem. This integration is performed by merging a GNSS solutions and lane centerline positions, acquired from aerial orthophotos, into a Kalman Filter and a simple map matching approach. To measure the positioning error, or off-track performance, a conversion of positions to the road space is necessary. To evaluate the results, a positioning accuracy limit, considering the road, vehicle dimensions, and the requirements for ITLBS is also proposed. The results showed that 95% of the time the proposed methodology off-track performances were within 1.89 m, in an average of 4 runs. Half of the runs were within 0.75 m, in average, at 95% of the time. Compared to an accurate GNSS Post Processed Kinematic (PPK) mode, an improvement of 10% was achieved.

Keywords

GNSS · ITLBS · Lane-level positioning · Maps

1 Introduction

Intelligent Transportation Systems (ITS) applications are rapidly emerging and efforts are being made in order to set appropriate standards. For example, positional accuracy

standards for Intelligent Transportation Location Based Services (ITLBS) technologies. A complete review on the accuracy for ITLBS was carried by Stephenson et al. (2011), where four main classes of accuracy categories were outlined: which road (5.0 m); which lane (1.5 m); where in lane (0.5 m); and active control (0.1 m).

GNSS has been the main system for providing consistent global positions in several applications. However, there are major issues limiting the ITLBS application requirements, such as availability, continuity, and integrity. It is conceivable that GNSS positions along with accurate map information

E. P. Cavalheri (✉) · M. C. dos Santos
Department of Geodesy and Geomatics Engineering,
University of New Brunswick, Fredericton, NB, Canada
e-mail: e.cavalheri@unb.ca; msantos@unb.ca

offers a potential worldwide autonomous driving without any other lane and road detection/identification sensors (Bishop 2005; Hillel et al. 2014).

When it comes to vehicle autonomous navigation systems and related applications, GNSS and maps are normally used separately for distinct purposes. One of the primary challenge in autonomous systems is the navigation, which basically requires an accurate knowledge of the vehicle's position in the environment. Current developments have mostly been using imagery sensors to identify the lanes. However, imagery systems always depend on light and well structured roads to correctly identify the edges of roads, leading to failures in dark or to bright environments (Hillel et al. 2014; Li et al. 2014).

Therefore, this work proposes an integration of GNSS and road map information to address this problem. This integration is performed by merging a GNSS position solution and lane centerline positions, from aerial orthophotos, into a Kalman Filter and a map matching algorithm. To measure the positioning error with respect to the reference lanes, a conversion of positions to the road space is necessary. To evaluate the results, a positioning accuracy limit, considering the road, vehicle dimensions, and the requirements for ITLBS is also proposed. In the following section, methodology, a satellite positions and map centerline approach using Kalman filter and a map matching algorithm will be outlined. In the sequence, in the section experiment and results, a study case describes the performance of the methodology followed by an statistical analysis of the off-track solutions, in the section analysis. And then, the conclusions of this work are discussed.

2 Methodology

This proposition integrates positions, from a satellite positioning technique, with the centerline position of the lanes, into a Kalman Filter, with the objective of keeping the estimated solutions in the center of lanes. At every satellite position solution (z_k), a map matching algorithm is executed to correctly identify where the vehicle is likely to be in the reference lanes (x_{ref}). By using this map-matched point (x_{mm}) and the lanes orientation, the filter prediction step ($\hat{x}_{k/k-1}$) is constrained to keep the next position and velocity state, estimated in the filter update step (\hat{x}_k), in the lane. The flowchart in Fig. 1 describes this procedure.

In the sequence, the map matching and kalman filter algorithms are detailed.

2.1 Map Matching

The main purpose of a map matching algorithm is to identify the correct road segments that a vehicle is travelling and its correct position on that segment (Quddus et al. 2003). Quddus et al. (2007) presented a complete review on the different MM algorithms and its performances. To mention a few techniques, map matching algorithms can range from simple geometric searching techniques, to complexes ones using fuzzy logic, Extended Kalman Filter (EKF), and Belief Theory. These techniques can be categorized into four main groups: geometric, topological, probabilistics, and advanced algorithms.

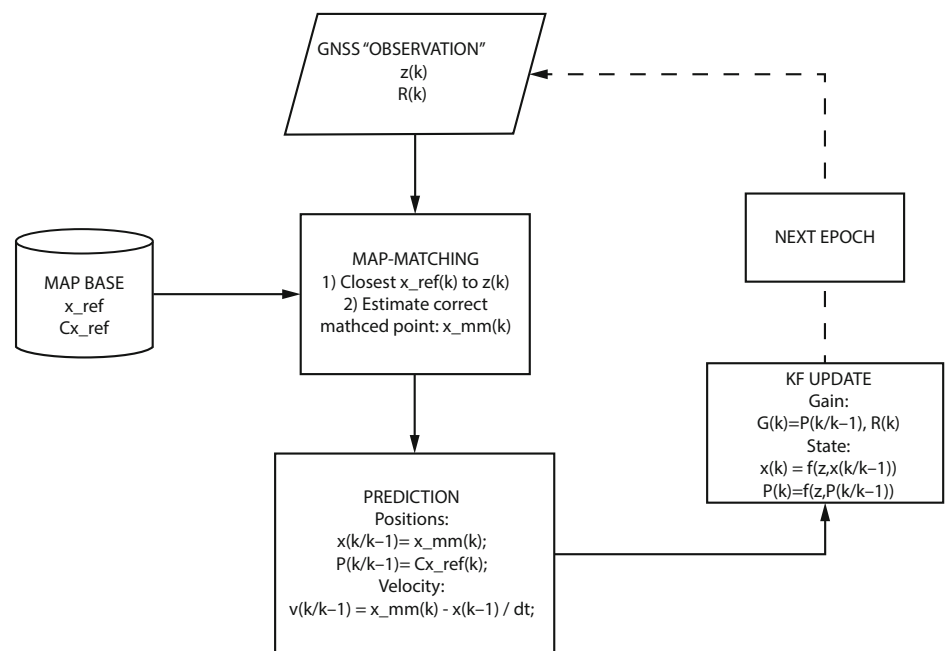


Fig. 1 Filter flowchart

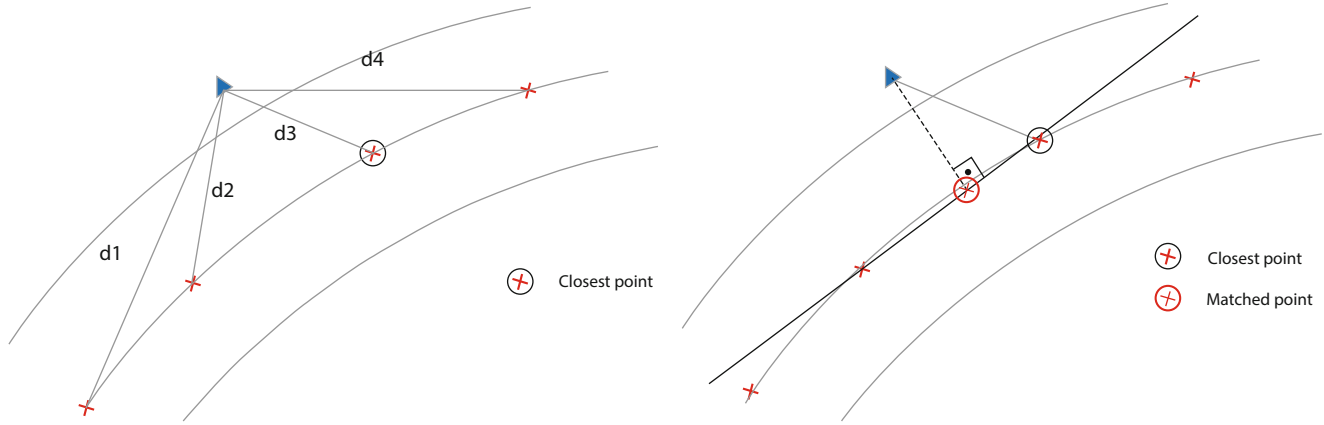


Fig. 2 Map matching step 1 (left) and step 3 (right)

The type of algorithm may be chosen depending on the type of data fed to the map matching process. In this work, positions coming from either the vehicle and the lane are used, therefore a simple geometric map matching is selected and explained in the sequence.

The first step of the map matching is to determine a position in the reference lane that is closest to the satellite position solution. This situation is depicted on the left side of Fig. 2, where the satellite position is represented as a blue triangle, the reference lane candidates as red crosses. The candidate with the shortest distance (d_i) to the satellite position is chosen as the closest point. Then, the second step is to fit a line equation in the reference lane neighbouring candidates so that a perpendicular projection of the satellite position can be made onto this line. The intersection of the projection in this line gives the map-matched position x_{mm} . The right side of Fig. 2 depicts this second step. For the sake of illustration the line fit is made over a well spaced candidate points, which results on a line being not in the lane centerline, however in the experiments, on a real scenario, the points spacing are close enough to consider the line as the adjusting geometry.

From this step, the map-matched position and line orientation, or azimuth, are used in the navigation filter, as it explained in the sequence.

It should be noted that in the experiments the map contains only the lanes where the vehicle navigated, thus road identification is not necessary in this map matching approach. This way, there is no concerns with road ambiguous selection, for instance in intersections.

2.2 Navigation Algorithm

The information extracted from the lanes are used to constrain the navigation filter. The mathematical model uses local coordinates and the horizontal position and the velocity

are the states to be estimated:

$$\begin{aligned} n_k &= n_{k-1} + v \cdot dt \cdot \cos(\theta) \\ e_k &= e_{k-1} + v \cdot dt \cdot \sin(\theta) \\ v_k &= v_{k-1} + w_k \end{aligned} \quad (1)$$

where, n, e are the local north and east components, v is the vehicle horizontal velocity, θ is the azimuth, w_k is the velocity process noise, and dt is the time between observations.

The Kalman Filter (KF) is an optimal estimation framework to solve the dynamic system presented in Eq. (1) (Grover and Hwang 1992). This system and measurement models can be represented in the following form, respectively:

$$\begin{aligned} \mathbf{x}_k &= \mathbf{F}_{k-1} \mathbf{x}_{k-1} + \mathbf{v}_{k-1} \\ \mathbf{z}_k &= \mathbf{H}_{k-1} \mathbf{x}_k + \mathbf{w}_k \end{aligned} \quad (2)$$

where \mathbf{x}_k is the state vector, \mathbf{F}_{k-1} and \mathbf{H}_{k-1} are the Jacobian matrices of the functions with respect to the state vector \mathbf{x}_k , of the state and measurement functions, respectively. The noise sequences \mathbf{v}_{k-1} and \mathbf{w}_k are assumed to be white with known probability density function and mutually independent, with respectively covariance matrices: \mathbf{Q}_{k-1} and \mathbf{R}_k .

The Kalman filter is a recursive process with the prediction and update steps. In the prediction step, the state and error covariance are estimated from previous timestep:

$$\begin{aligned} \hat{\mathbf{x}}_{k/k-1} &= \mathbf{F}_{k-1} \hat{\mathbf{x}}_{k-1} + \mathbf{v}_{k-1} \\ \mathbf{P}_{k/k-1} &= \mathbf{Q}_{k-1} + \mathbf{F}_{k-1} \mathbf{P}_{k-1} \mathbf{F}_{k-1}^T \end{aligned} \quad (3)$$

where \mathbf{P}_k is the state error covariances.

In this proposition, the state vector prediction is provided by the map matching (x_{mm}). The navigation orientation (θ), which will impact the matrix \mathbf{F}_{k-1} , is obtained from the map. This quantities along with the measurements (\mathbf{z}_k), the vehicle positions in this case, are the inputs for the Kalman

filter update:

$$\begin{aligned}\hat{\mathbf{x}}_k &= \hat{\mathbf{x}}_{k/k-1} + \mathbf{K}_k(\mathbf{z}_k - \mathbf{H}_k \hat{\mathbf{x}}_{k/k-1}) \\ \mathbf{P}_k &= (\mathbf{I} - \mathbf{K}_k \mathbf{H}_k) \mathbf{P}_{k/k-1}\end{aligned}\quad (4)$$

where $\mathbf{K}_k = \mathbf{P}_{k/k-1} \mathbf{H}_k^T (\mathbf{H}_k \mathbf{P}_{k/k-1} \mathbf{H}_k^T + \mathbf{R}_k)^{-1}$ is the Kalman gain.

The dynamics of the problem is a car navigating in the streets of a city and according to tests made by Hu et al. (2003), 0.1 m/s^2 were the best dynamic noise for this situation and is the value considered in this work. For details on the application of the Kalman filter several textbooks or papers provides its flow (Miller and Leskiw 1987; Hu et al. 2003; Ristic et al. 2004).

2.3 Positioning Accuracy Limit

The position errors with respect to the lane centerline should be within a limit to evaluate the methodology. An accuracy threshold that considers the vehicle (v_w) and lane (l_w) dimensions is proposed and depicted in Fig. 3.

Considering the average lane sizes where vehicle navigates and the vehicle lateral widths, the following lane threshold can be developed,

$$\sigma_{lim} = (l_w/2) - (v_w/2) \quad (5)$$

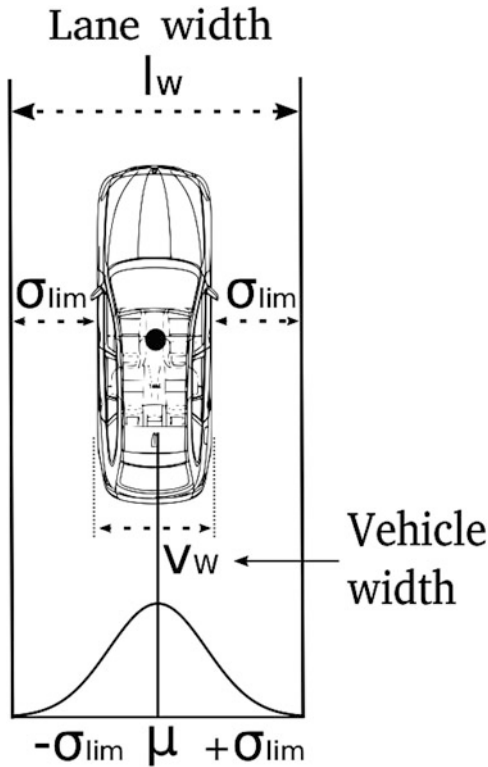


Fig. 3 Vehicle navigation threshold

The threshold σ_{lim} represents the very limit of the lane, to be more conservative, an appropriate value for a safer limit would be $\sigma_{lim}/2$. For this experiment, the accuracy threshold value is $\sigma_{lim}/2 = 0.49 \text{ m}$.

3 Experiment and Results

A satellite dataset was collected in the streets of Fredericton, New Brunswick, Canada. Two geodetic dual-frequencies receivers were mounted on the roof of a vehicle for the collections. The position solution was obtained from a post-processed kinematic (PPK) technique with a short baseline station ($<8 \text{ km}$). The data was processed using the open source RTKlib package for satellite positioning, details can be seen at Takasu (2018). The road centerlines positions were digitized from a 15-cm resolution orthophotos provided by the city of Fredericton. The positions representing the trajectory were generated at every 0.5 m in the road centerline. The dataset was processed separately for each receiver thus the solutions are seen separately.

In a first moment, position performances will be visualized during GNSS outages. In Figs. 4 and 5, the estimated positions of the vehicle using the Kalman filter (as green stars) and the PPK solution (colored circles) are visualized along with the reference lane centerlines (yellow dots). The same stretch of the road are seen for receiver 1 and 2 respectively at the left and right side of the figures.

Figure 4 show the filter performance after a complete and quick outage when the vehicle passed underneath a walking bridge. The direction of navigation is from the bottom to the upper part of the figures. After the complete outage, the PPK solution suffers a quick reconvergence and can only determine a position using the low accurate pseudorange observable, also known as single point positioning (SPP, represented as red circles). The KF solution showed a better performance where it kept the position correctly on the lane before and even after the outage.

Figure 5 shows the vehicle coming from the upper part and taking the exit ramp and passing underneath the bridge. Both receiver solutions have similar behaviours. The RTK and KF solutions are practically together before passing under the bridge. After the complete signal blockage, PPK solutions went away of the lane of navigation while the KF solutions were mostly in right lane of navigation. It is observed when PPK solutions are float the filter trusts more the road centerline information. However, when the PPK solution fix ambiguities, thus with a small standard deviation, the filter trusts more the GNSS positions.

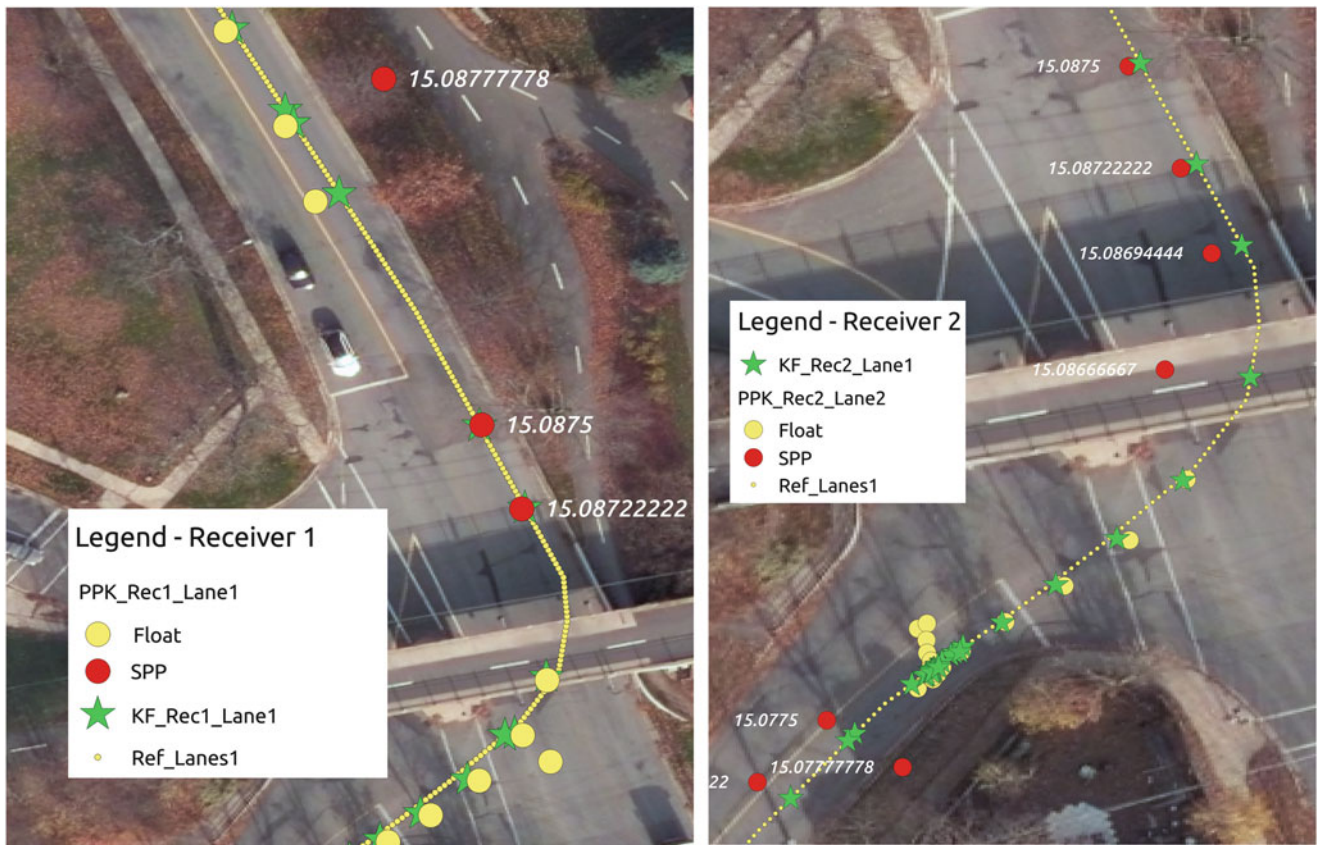


Fig. 4 Receivers 1 (left) and 2 (right) KF (green stars) and PPK (circles) performances passing underneath a walking bridge

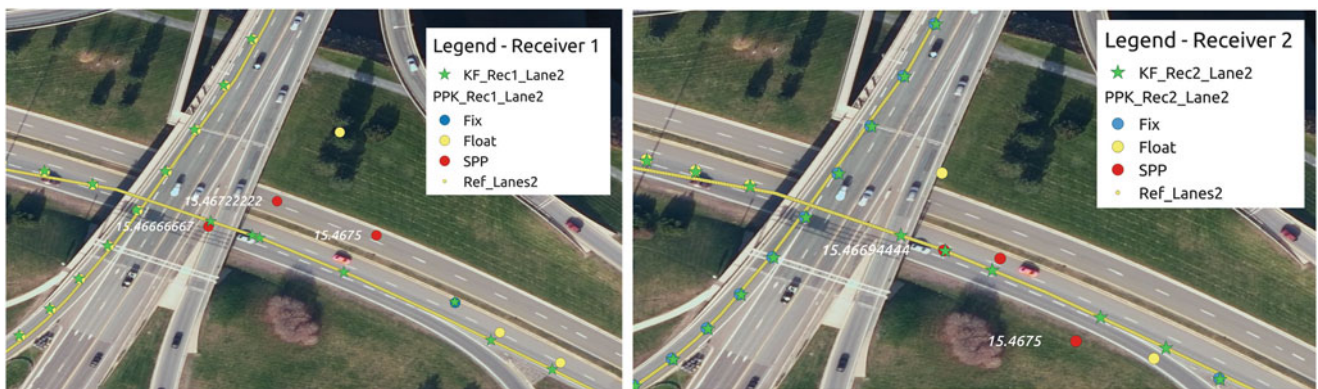


Fig. 5 Receivers 1 (left) and 2 (right) KF (green stars) and PPK (circles) performances passing underneath a walking bridge

One delicate situation was noticed when the vehicle passed inside a urban canyon where the occurrence of multipath was high. During this situation the receiver observes measurements from reflected signals which makes the filter to determine with confidence a wrong position. This situation is seen in Fig. 6, in which a wrong PPK fix misled the Kalman filter solution, which judged the position as being correct.

4 Analysis

The methodology is assessed by determining the off-track of PPK and KF solutions to the reference lanes, for both receivers 1 and 2. The processing was separated by the navigation direction, going to the halfway trajectory point (Lanes 1) and coming back to the starting point (Lanes 2), visualized in Fig. 7.



Fig. 6 Wrong filter positioning due to a wrong GNSS position fixes on a urban canyon

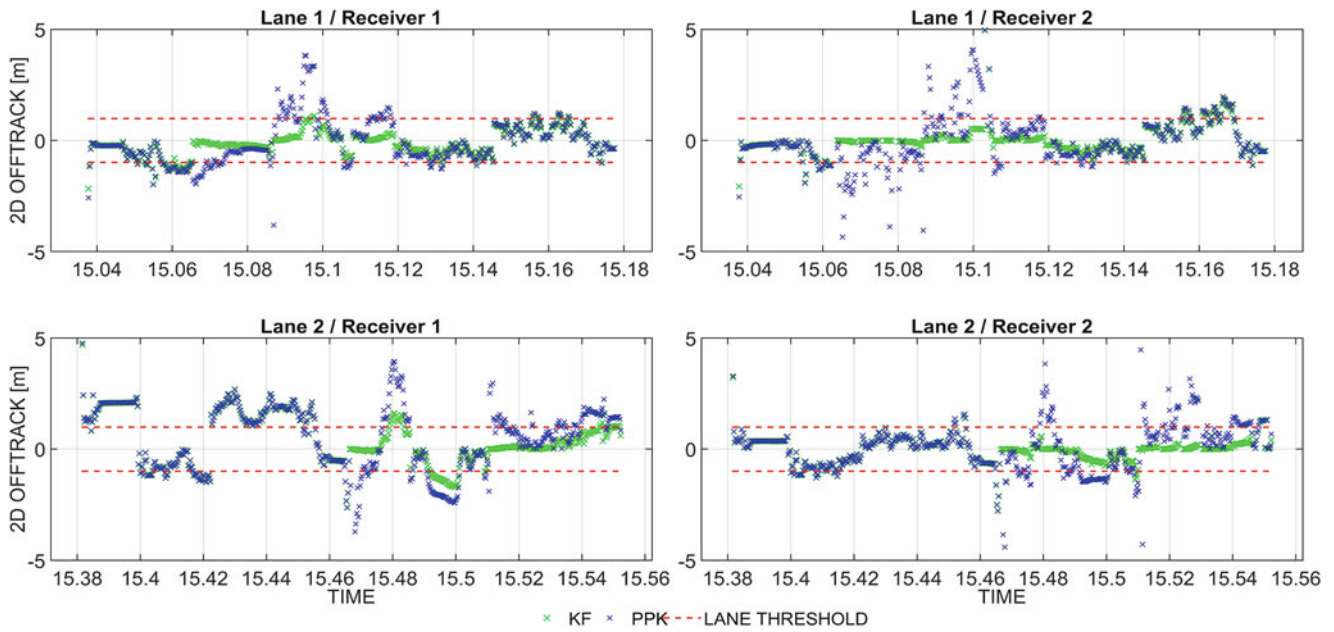


Fig. 7 Off-track for receivers 1 (left) and 2 (right) in the lanes 1 (top) and 2 (bottom)

Table 1 Off-track accuracy analysis

PPK			KF		
avg (m)	std (m)	95% (m)	avg (m)	std (m)	95% (m)
0.74	0.70	2.10	0.56	0.58	1.89

Statistics of the off-track measure were grouped for both receivers into one, and are shown as the average off-track (avg), its standard deviation (std), at 95% confidence level for PPK and KF solutions, in Table 1. Satellite obstructions were disregarded in the statistics due to the great impact in the PPK solutions.

The results showed that 95% of the time the KF off-track performances were within 1.89 m in average for the 4 runs, while PPK had an average of 2.10 m. An improvement of 10% KF had over the PPK off-track performances. Considering the lane threshold standard deviation proposed in this work for the off-track evaluation, $\sigma_{lim} = +/- 0.49$ m, the KF average performance was 0.56 m, only 7 cm above the limit. However, when considering 95% of the data, the KF solutions were 1.88 m, more than 3 times the limit. The PPK mean was above the limit for 25 cm. And, 95% of the data were under 2.09 m. This way, for the required limit of 0.49 m, the proposed methodology did not achieve the active control limit 95% of the time.

5 Conclusion

This work proposed an integration of GNSS positions and lane centerlines into a Kalman Filter and map matching approach, with the main objective of keeping the vehicle position in the lane center. Mostly, the KF off-track performances follows the PPK solution. The main limiting points are the long periods of GNSS outages affecting the quality of the KF positions and wrong PPK fixed positions due to multipath. The improvements obtained by the approach are during short and complete signal outages where the map aids the filter with the satellite observations blockages making a continuous solution while keeping it in the correct lane.

The concern from the community towards low-cost single frequency navigation systems was reasonable few years ago, however, in a few years from now, the cost versus performance of dual frequencies against single frequency receivers will be justified as the prices lower and the need for performance increases especially for safety of life navigation applications.

The main challenges for future tests is to develop a filter that integrates the map information with satellite measurements to exclude wrong fixes due to multipath signals and improve the solution continuity in any duration of satellite outages.

Acknowledgements To the CNPq (Conselho Nacional de Desenvolvimento Científico e Tecnológico) agency, which through the Brazilian

Sciences without borders program provided the necessary funds for the development of this research.

References

- Bishop R (2005) Intelligent vehicle technology and trends. Artech House, Boston
- Grover R, Hwang PYC (1992) Introduction to random signals and applied Kalman filtering. Wiley, New York
- Hillel AB, Lerner R, Levi D, Raz G (2014) Recent progress in road and lane detection: a survey. *Mach Vis Appl* 25(3):727–745
- Hu C, Chen W, Chen Y, Liu D (2003) Adaptive Kalman filtering for vehicle navigation. *J Glob Positioning Syst* 2(1):42–47
- Li Q, Chen L, Li M, Shaw SL, Nuchter A (2014) A sensor-fusion drivable-region and lane-detection system for autonomous vehicle navigation in challenging road scenarios. 63(2):540–555
- Miller KS, Leskiw DM (1987) An introduction to Kalman Filtering with applications. Riverside Research Institute, New York
- Quddus MA, Ochieng WY, Zhao L, Noland RB (2003) A general map matching algorithm for transport telematics applications. *GPS Solut* 7(3):157–167
- Quddus MA, Ochieng WY, Noland RB (2007) Current map-matching algorithms for transport applications: state-of-the art and future research directions. *Transp Res Part C: Emerg Technol* 15(5):312–328
- Ristic B, Arulampalam S, Gordon N (2004) Beyond the Kalman filter: particle filters for tracking applications. Artech House, Boston
- Stephenson S, Meng X, Moore T, Baxendale A, Ford T (2011) Accuracy requirements and benchmarking position solutions for intelligent transportation location based services. In: Proceedings of the 8th international symposium on location-based services
- Takasu, T (2018) RTKLIB: An open source program package for GNSS positioning (2018-07-11). <http://www.rtklib.com>